University of Vienna
Faculty of Physics

Tutorial Material

Praktikum:
Bell´s Inequality

Chiara Greganti **Lorenzo Procopio**

2013/2014

Contents

Safety guidelines

Before beginning an optics experiment, one must read and abide by the following safety rules and general conditions [14]:

- Do not enter in the lab with food or drinks.
- The laser used has a maximum power of $50mW$. To prevent damage to the eyes because of laser beam and its possible unexpected refractions, it is mandatory to wear safety goggles.
- Never look directly into the beam.
- During the experiment, the head should not be ends at table height. It should be omitted even possible to bend down to the ground (otherwise: close your eyes).
- No possible reflective ornaments and belts, as well as any accessories (rings, necklaces , watches or similar) may be worn.
- All the optical components are very sensitive: lenses, mirrors, crystals , filters, etc. must not be touched.
- Quantum optics set-up is very sensitive. Every optical components must therefore always be screwed.
- The optical fibers must not be removed from the detector module. Always keep a dust cap on a fiber optic cable when it is not in use.
- Always switch off the light for a dark room before starting to use the single-photon avalanche photodiodes. Too much exposure to light can damage them.

Chapter 1

Bell´s Inequality Theory

1.1 History

The history of the Bell inequalities begins with a paper published by Einstein, Podalsky and Rosen (EPR) in 1935 [3]. The EPR paper was intended to be a positive step towards showing the existence of a more objective reality beyond the statistical superposition described by quantum mechanics. They claimed that the paradox could be explained by the existence of some unknown physical quantity, so-called hidden variable, which quantum mechanics miss completely. Therefore reaching the conclusion that quantum mechanics is an *incomplete* theory.

In 1964 J.S. Bell published a theorem in the form of an inequality which holds for all local hidden variable theories and is incompatible with quantum mechanical prediction [4]. For the first time they developed a quantitative argument. Testing the inequality, the principle of locality stands to fail rather than quantum mechanics. Indeed, tests of Bell's inequality have shown violations of the conditions to which all local hidden variable theories must adhere. Other like-Bell inequalities have been proposed [21], but the so-called CHSH-Bell inequality (see sec. 1.4) is very handy to implement in many experiments.

The first experimental test and generalization of Bell's inequality were performed by Stuart J. Freedman and John F. Clauser in 1972 [5]. They measured the linear polarization correlation of the photons emitted in atomic cascade of calcium. Aspect, Grangier, and Roger realized subsequent experimental tests in 1981 giving a new violation of Bell's Inequalities [6]. Z. Y. Ou and L. Mandel reported in 1988 the violation of Bell's inequality using correlated photons produced in the process of parametric down-conversion (SPDC) [7]. Kwiat *et. al*. developed better and brighter source of polarization entangled photons based on SPDC [8]. They demonstrated a violation of Bell's inequality by over 100 standard deviations using down-converted photons.

1.2 Entanglement

Entanglement is an intriguing, direct consequence of quantum mechanics formalism [9]. The Hilbert space of a composite quantum system is the tensor product of its

subsystem spaces. For a system of two particles, whose quantum states are $|0\rangle_i$ and $|1\rangle_i$ where $i = 1, 2$, we say that the the system is entangled when the state of the system $|\psi^+\rangle$ cannot always be written as the tensor product of its subsystem:

$$|\psi^+\rangle = \frac{1}{\sqrt{2}}(|0\rangle_1|1\rangle_2 + |1\rangle_1|0\rangle_2) \neq (a|0\rangle_1| + b|1\rangle_1|)(a|0\rangle_2| + b|1\rangle_2). \tag{1.1}$$

where a and b are complex numbers. The entangled states that form the basis for two qubits are the four so-called *Bell*, or *EPR*, states:

$$|\psi^\pm\rangle = \frac{1}{\sqrt{2}}(|0\rangle_1|1\rangle_2 \pm |1\rangle_1|0\rangle_2) \tag{1.2}$$
$$|\phi^\pm\rangle = \frac{1}{\sqrt{2}}(|0\rangle_1|0\rangle_2 \pm |1\rangle_1|1\rangle_2)$$

It is easy to see that the Bell states are not separable and therefore entangled, according to our definition. They represent the most basic form of entangled states and describe the correlations between two entangled qubits 1 and 2.

1.3 Bell's inequality

The EPR paradox was given as an argument that quantum mechanics could not be a complete theory* but should be supplemented by additional variables. These additional variables were to restore the theory causality and locality [4].

The Bell's inequality is based in two assumptions: (i) *reality*, that microscopic objects have real properties determining the outcomes of quantum mechanical measurements, and (ii) *locality*, that reality in one location is not influenced by measurements performed simultaneously at a distant location.
Bell considered a pair of spin-1/2 particles formed in the singlet spin state

$$|\psi\rangle = \frac{1}{\sqrt{2}}(|\uparrow\rangle_1|\downarrow\rangle_2 - |\downarrow\rangle_1|\uparrow\rangle_2), \tag{1.3}$$

where $|\uparrow\rangle$ ($|\downarrow\rangle$) is the spin component +1 (-1) in the direction z. Measurements can be made along arbitrary directions $\vec{a}$ and $\vec{b}$, with $|\vec{a}| = |\vec{b}| = 1$. This corresponds to apply the operators $\vec{\sigma}_1 \cdot \vec{a}$ and $\vec{\sigma}_2 \cdot \vec{b}$, where $\vec{\sigma} = \hat{\sigma}_x, \hat{\sigma}_y, \hat{\sigma}_z$ and $\hat{\sigma}_x, \hat{\sigma}_y, \hat{\sigma}_z$ are the Pauli matrices. If one measures both particles along the same axis $\vec{a}$, the results are anti-correlated, i.e. if for $\vec{\sigma}_1 \cdot \vec{a}$ the measured value yields 1 then for $\vec{\sigma}_2 \cdot \vec{a}$ the measured value must be -1 and vice versa. It is assumed that the measurements are carried far away from each other and will not affect each other (locality). For a local realistic interpretation of entanglement Bell introduces the dependence on a hidden variable λ, which could be a single variable or a set of variables. The values of λ affect the measurements of the entangled particles and vary according to unknown rules, but are distributed according to a probability $\rho(\lambda)$, where

$$\rho(\lambda) \geq 0 \quad \text{where} \int \rho(\lambda) d\lambda = 1. \tag{1.4}$$

Completeness is defined by: "every element of physical reality must have a counterpart in the physical theory."

The measurement result of $\vec{\sigma}_1 \cdot \vec{a}$ is then determined by $\vec{a}$ and λ, $A(\vec{a}, \lambda)$, and in the same instance the measurement result of $\vec{\sigma}_2 \cdot \vec{a}$ by $\vec{b}$ and λ, $B(\vec{b}, \lambda)$, so that

$$A(\vec{a}, \lambda) = \pm 1, \qquad B(\vec{b}, \lambda) = \pm 1. \tag{1.5}$$

The vital assumption (locality) is that the result B for particle 2 does not depend on the setting $\vec{a}$, of the magnet for particle 1, nor A on $\vec{b}$. The expectation value of the product of two components $\vec{\sigma}_1 \cdot \vec{a}$ and $\vec{\sigma}_2 \cdot \vec{b}$ is then

$$E(\vec{a}, \vec{b}) = \int d\lambda \rho(\lambda) A(\vec{a}, \lambda) B(\vec{b}, \lambda). \tag{1.6}$$

P cannot be less than -1. It can reach -1 at $\vec{a} = \vec{b}$ only if

$$A(\vec{b}, \lambda) = -B(\vec{b}, \lambda) \qquad \Rightarrow \qquad E(\vec{a}, \vec{b}) = -\int d\lambda \rho(\lambda) A(\vec{a}, \lambda) A(\vec{b}, \lambda) \tag{1.7}$$

Considering $\vec{c}$ another unit vector, it follows that:

$$E(\vec{a}, \vec{b}) - E(\vec{a}, \vec{c}) = \int d\lambda \rho(\lambda) A(a, \vec{\lambda}) A(\vec{b}, \lambda)[A(\vec{b}, \lambda) A(\vec{c}, \lambda) - 1], \tag{1.8}$$

where $A(\vec{b}, \lambda)^2 = 1$ is used. Considering the modulus on both sides and the triangle inequality, one finds:

$$\mid E(\vec{a}, \vec{b}) - E(\vec{a}, \vec{c}) \mid \leq 1 + E(\vec{b}, \vec{c}). \tag{1.9}$$

This is the famous Bell's inequality which every local hidden variable must satisfy.

1.4 CHSH-Bell inequality

Bell's result relies on the assumptions of perfect (anti-)correlations and error-free measurement devices. However none of the two cannot be implemented in real-world experiments. So John Clauser and *et al* derived a generalization of the equation 1.9 in such a way it "depends continuously" on the correlations. They wrote down a mathematically precise formulation of a consequence of locality in the context of an experiment in which measurements are performed on two systems which have previously interacted, but which are now spatially separated. The outcomes exhibit statistical regularities, i.e. they are governed by probability distributions depending on the experiments performed and in particular on the setting of measurements, α and β. In this way CHSH-Bell inequality gives classical limits to the expected correlation between two parts.

We define the correlation $E(\alpha, \beta)$ as the expected value of the product of the two observables A and B for a given choice of setting α and β:

$$E(\alpha, \beta) = \int d\lambda \rho(\lambda) A(\alpha, \lambda) B(\beta, \lambda). \tag{1.10}$$

We can derive an upper limit for all possible values by manipulation this expression in the following way:

$$
\begin{aligned}
E(\alpha',\beta)+E(\alpha',\beta') &= \int d\lambda\rho(\lambda)[A(\alpha',\lambda)B(\beta,\lambda)+A(\alpha',\lambda)B(\beta',\lambda)] \\
&= \int d\lambda\rho(\lambda)[A(\alpha',\lambda)B(\beta,\lambda)+A(\alpha',\lambda)B(\beta',\lambda)+ \\
&A(\alpha,\lambda)B(\beta',\lambda)A(\alpha',\lambda)B(\beta,\lambda)-A(\alpha,\lambda)B(\beta,\lambda)A(\alpha',\lambda)B(\beta',\lambda)] \\
&= \int d\lambda\rho(\lambda)[A(\alpha',\lambda)B(\beta,\lambda)(1+A(\alpha,\lambda)B(\beta',\lambda)) \\
&+A(\alpha',\lambda)B(\beta',\lambda)(1-A(\alpha,\lambda)B(\beta,\lambda))]
\end{aligned}
\tag{1.11}
$$

so

$$
\begin{aligned}
|E(\alpha',\beta)+E(\alpha',\beta')| &\leq \Big|\int d\lambda\rho(\lambda)(1+A(\alpha,\lambda)B(\beta',\lambda))\Big|+\Big|\int d\lambda\rho(\lambda)(1-A(\alpha,\lambda)B(\beta,\lambda))\Big| \\
&= 2+|E(\alpha,\beta')-E(\alpha,\beta)|
\end{aligned}
\tag{1.12}
$$

where in the last line we considered the absolute values of all the independent components. The Bell parameter is then defined as:

$$
S(\alpha,\alpha',\beta,\beta')=|E(\alpha,\beta)-E(\alpha,\beta')|+|E(\alpha',\beta)+E(\alpha',\beta')|\leq 2 \tag{1.13}
$$

For the experiment considered above with a singlet state $|\psi^-\rangle$, quantum theory predicts $E(\alpha,\beta) = -\alpha\cdot\beta$ (where the $\cdot$ denotes the Euclidean inner product and the oriented axes α, β are identified with their corresponding unit vectors and therefore $E(\alpha,\beta) = -\cos(\alpha-\beta)$ [14]). For this experiment, the CHSH-Bell inequality is maximally violated by the quantum predictions if β and β' are mutually orthogonal, α' bisects β and β', and α bisects β and the opposite axis $-\beta'$ (e.g. taking the setting of angles $\alpha=0,\beta=\frac{\pi}{4},\alpha'=\frac{\pi}{2},\beta'=\frac{3\pi}{4}$). In that case, $S=2\sqrt{2}$.

1.5 Loopholes

A loophole is an ambiguity in a statement which can be used to circumvent or avoid the purpose of such statement. The main loopholes in Bell's inequalities are:

1. *Locality loophole*. It arises when the measurement results on one system can be influenced by a measurement - or by the setting choice event (the choice of which measurement will be performed) - on a second spatially separated system, and vice versa. This loophole was closed by Alain Aspect's experiments [6].

2. *Freedom-of-choice loophole*. Freedom of choice means that the setting choices must themselves be free of any potential influence by the event which created the two systems in the first place. In other words, similar to above, the choice of measurement settings, in practice generated by a quantum random number generator (which is another crucial requirement), has to occur outside of the future light cone of the event that created the two (entangled) systems and hence imprinted the hidden variable on them. This loophole was closed by Shiedl (2010) [10].

3. *Fair-sampling (detection) loophole*. It states that classical, rather than quantum, effects could be responsible for measured correlations between entangled pairs of photons. Also this loophole was closed recently [11].

The loopholes are important for quantum foundations and for security of entanglement-based quantum cryptography [12].

Chapter 2

Photonic Bell´s Inequality Experiment

To test the Bell Inequality´s violation in an experiment, the physical systems of choice are single photons. Photon polarization is used as two-level quantum system, in particular we associate horizontal (H) and vertical (V) polarizations to σ_Z basis states:

$$\{|0\rangle, |1\rangle\} \equiv \{|H\rangle, |V\rangle\}. \tag{2.1}$$

Here we present all the main elements necessary to implement the photonic experiment. Mostly this chapter is based on R. Prevedel´s thesis [2] and Y. Nazirizadeh´s thesis [15].

2.1 Entangled Photons Production

Generation of single photons in pure quantum states is achieved - nowadays mainly - by the process of spontaneous parametric down-conversion (SPDC) [16, 17].

This process takes place in non-linear optical materials, such as anisotropic or non-centrosymmetric crystals. Technically, the nonlinearity of the materials is reflected in the dielectric polarisation vector, P. When an electromagnetic field such as the light field of a laser interacts with a dielectric medium, it induces electric dipole moments, whose macroscopic sum results in an induced dipole polarization $\overrightarrow{P}$ inside the material. Its components P_i are related to the electromagnetic field $\overrightarrow{E}$ and can be written as a series expansion [16],

$$P_i = \epsilon_0(\chi^{(1)}_{ij} E_j + \chi^{(2)}_{ijk} E_j E_k + \chi^{(3)}_{ijkl} E_j E_k E_l \ldots), \tag{2.2}$$

where ϵ_0 is the permittivity of the vacuum, $\chi^{(1)}$ ($\approx O(1)V/m$) is the standard linear coefficient of dielectric susceptibility and E_i denotes the components of the electric field. The contribution of the nonlinear second-order term ($\chi^{(2)} \approx O(10^{-10})V/m$)) in 2.2 is usually neglected for weak pump fields. At sufficiently high electric field strength however it becomes significant, eventually leading to oscillator terms which are driven by twice the frequency of the incident fields (second harmonic generation process, SHG) or to the reverse process (SPDC).

2.1.1 Birefringence

In many non-linear optical materials the index of refraction depends on the direction of the electric field vector. Birefringent* materials can be characterized by two indices of refraction, one for ordinary (*o*-) rays and one for purely extraordinary (*e*-) rays. The *optic axis* of a birefringent material is the direction along which a ray of any polarization will travel at the same speed, without suffering of double refraction effect. An ordinary ray has polarization orthogonal to the plane spanned by the optic axis and the direction of the incident electric field vector, while a purely extraordinary ray has polarization parallel with this plane. The ordinary ray is subject to the ordinary index of refraction, n_o,while $\overline{n}_e$ is the index of refraction for the extraordinary ray. Rays with polarization in the plane of the optic axis propagate according to an effective index of refraction n_e given by the relation

$$\frac{1}{n_e(\theta)^2} = \frac{sin(\theta)^2}{\overline{n}_e(\theta)^2} + \frac{cos(\theta)^2}{n_o(\theta)^2}, \tag{2.3}$$

where θ is the angle between the optic axis and propagation direction (Fig. 2.1). In general materials are dispersive, and $\overline{n}_e = \overline{n}_e(\lambda)$ and $\overline{n}_o = \overline{n}_o(\lambda)$, where λ is the wavelength, are given by the Sellmeier equations. Birefringent materials are called negative or positive according to the sign of $\overline{n}_e - n_o$ s[16]. For negative birefringent crystal, such as BBO (β-barium borate - β-BaB_2O_4), the ordinary constituent of the beam travels faster than the extraordinary one ($n_o > n_e$).

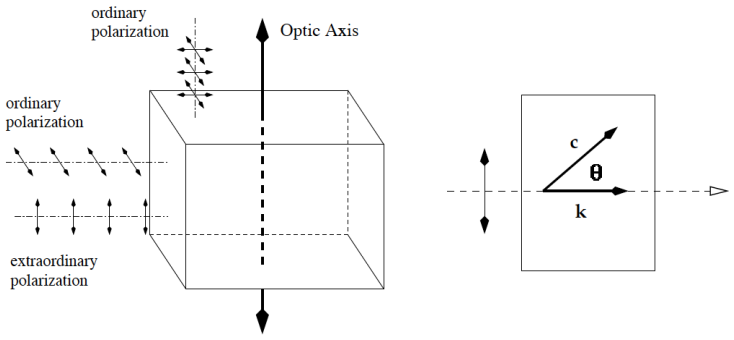

Figure 2.1: The optical geometry of birefringence. On the left diagram of a birefringent material showing the relative geometry of ordinary and extraordinary rays with the optical axis. On the right a wave polarized in the plane defined by the optic axis c and its propagation vector k has an effective index of refraction related to n_o, $\overline{n}_e$ and θ. See eq. 2.3. Figure taken from [18].

2.1.2 SPDC

In terms of photons, i.e. in the language of second quantization, SPDC process corresponds to the spontaneous conversion of a pump photon (p) with energy $\hbar\omega_p$ and momentum $\hbar\overrightarrow{k}_p$ into two photons with energies $\hbar\omega_s$, $\hbar\omega_i$ and momenta $\hbar\overrightarrow{k}_s$, $\hbar\overrightarrow{k}_i$,

*Birefringence is the optical property of a material having refractive index that depends on the polarization and propagation direction of light. It is responsible for the phenomenon of double refraction whereby a ray of light, when incident upon a birefringent material, is split by polarization into two rays taking slightly different paths.

where the $\overrightarrow{k}$ are the wavevectors inside the medium and s and i correspond to the down-converted photons, respectively *signal* and *idler*. This process is considered as a pure quantum effect [1].

In every parametric process energy and momentum are conserved for the three photons interacting in a non-linear medium, following the so-called *phase matching* conditions. In SPDC these conditions read like [17]

$$\omega_p = \omega_s + \omega_i \tag{2.4}$$

$$\overrightarrow{k}_p \approx \overrightarrow{k}_s + \overrightarrow{k}_i. \tag{2.5}$$

The pairwise generated photons are strongly correlated in their energy and momentum. Especially, the Eq. 2.5 implies that the SPDC emission is rotationally symmetric, which leads to a conic emission (see Fig. 2.2). For uniaxial crystals, depending on θ (i.e. how the crystal is cut[†]) two possible types of phase matching can be distinguished according to the polarization (combinations) of the down converted photons: if we have an e-polarized pump creating two o-polarized down-conversion photons, then it is called $type-I$, while an e-polarized pump creating one e- and one o-polarized photon is known as $type-II$ phase matching[‡].

In this Lab we choose to produce entangled photon using the process SPDC type-II with a BBO crystal (see Appendix A for specific parameters.)

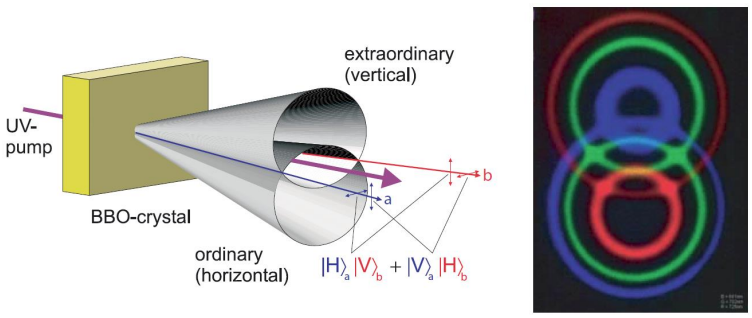

Figure 2.2: Principle scheme of type-II parametric down-conversion . On the right hand side, one can see the energy (i.e wavelength) dependent opening of the cones and the respective intersections. Entangled photon pairs are emitted in case where the photons are degenerate in frequency. Picture by P.G. Kwiat and M. Reck [8].

Since we require the photons to be indistinguishable in any degree of freedom other than spatial mode and polarization, we further choose the energies (or wavelengths) of both the signal and idler photons to be degenerate, which implies $\omega_s = \omega_i = \omega_p/2$.

The birefringence of non-linear crystals leads to a polarization dependent non-concentric splitting of the cones, as shown in Fig 2.2, where the opening angle of each cone depends on the angle enclosed by the pump wave vector and the principal axis of the crystal. This distinct emission geometry is known as $non-collinear$ and allows to have polarization-indistinguishable photons only on the intersection lines of the two cones, spatial mode a and b. When photons are emitted in these modes, it

[†]The crystal is cut such that light impinging perpendicular to the crystal's face forms an appropriate angle θ with the optic axis so that the down-converted photons obey the momentum conversation

[‡]Of course it is also possible for an o-polarized pump beam to generate either type of down-conversion.

becomes impossible, in principle, to tell whether the photon was emitted by the *o*- or *e*-cone, and because they correspond to different polarization, the photons become polarization entangled. In practice though, due to group velocity mismatch (negative birefringence of the crystal) the two photons exhibit slightly different propagation behaviour which renders them partially distinguishable - this has to be compensated in order to obtain genuine and high-quality entangled photons. Experimentally this is done by sending the photons through so-called compensation crystals, usually the same type of birefringent crystal, but of just half the thickness. If we further interchange the roles of ordinary and extraordinary beam before the compensators by rotating the polarization by 90°, the temporal and spatial walk-off will be canceled on average (see [14] for more details). One intuitive explanation is that by employing this method the information about the arrival time of the photon is erased, as can be seen schematically in Fig. 2.3. If this walk-off compensation is properly done, then the SPDC emission along modes a and b is an entangled state of the form

$$|\psi\rangle = \frac{1}{\sqrt{2}}(|V\rangle_a|H\rangle_b + e^{i\phi}|H\rangle_a|V\rangle_b). \tag{2.6}$$

The phase ϕ between the two coherent terms can be easily adjusted by introducing additional birefringent elements, or by slightly tilting one of the compensation crystals. In the experiment, choosing $\phi = 0°$ or $\phi = \pi$ will result in the maximally entangled Bell states $|\psi^+\rangle$ and $|\psi^-\rangle$, respectively. If additionally the polarization in one mode is rotated by 90°, any of the four distinct Bell states can be generated.

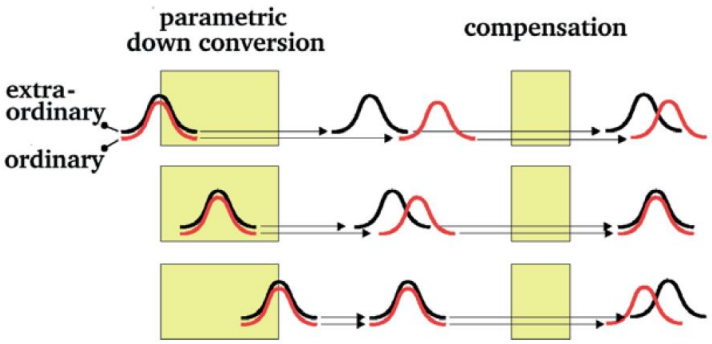

Figure 2.3: Since PDC is a spontaneous process, the down-conversion of the pump photon is equally probable at any point within the crystal. Therefore, the temporal delay between a horizontally and a vertically polarized photon varies depending on the crystal thickness and the point of down-conversion inside the crystal. By inserting compensators of half the thickness, one can, in average, delay the faster photon to erase this timing information. The additional HWPs in front of the compensators are not shown for clarity. Figure from [2].

Tip *In order to achieve high photon pairs emission from SPDC, we must focus the pump beam to the non-linear crystal, following Gaussian Optics (see Appendix B). This is done using a converging lens with precise focal length f (e.g. $f = 40mm$), displaced at the distance f before the crystal.*

Tip *In order to control and manipulate the polarization of a light beam, a quartz half wave plate (HWP) and quartz quarter wave plate (QWP), mounted on a rotary stages, are used according to the polarization angle of the incident and desired output light. Rotation of the HWP optic axis by θ relative to the polarization direction of the laser will result in*

a rotation by 2θ of the laser polarization angle. Rotation of the QWP optic axis allows to consider circular polarization. See Appendix C.

2.2 Photons Collection-Detection

2.2.1 SPCM

Single photons are coupled into fiber optic cables (single-mode fibers) ( ) and passed through these to a detection module, that counts the individual photons and indicates coincidences. A coincidence event is the result of two photons created at the same instant by downconversion and corresponds to detect polarization entangled photon pairs.

In the detection module two photodiodes are able to acquire single photons with an efficiency of about 40% light at $789nm$. They are often called single photon counting modules (SPCM). The photodiodes are very sensitive and expensive, and so must be used with great caution. At higher count rates the detectors will be damaged due to diode self-heating. To avoid detector overload, the detectors should only be operated in low-level lighting conditions. In addition narrow-band interference filters ($3nm$) are used in front of every detector, in conjunction with lenses which focus the beam onto the detection area. The filters are easy to remove in order to allow alignment by shining a laser pointer through the collector in reverse.

The SPCM output signal is amplified, processed and registered by a coincidence logic. This logic is configured and read-out by a personal computer. The coincidence (time) window, within which two or more incoming signals are considered to be coincident, is fixed at $6ns$.

2.3 Measurements and analysis

Violating the Bell´s Inequality requires measuring the quantum states in different basis. In the experiment this is related to measure the correlated photons in different polarization basis.

We define first the eigenstates of σ_x and σ_y basis, respectively corresponding to diagonal and circular polarizations, as:

$$|D/A\rangle = \frac{1}{\sqrt{2}}(|H\rangle \pm |V\rangle) \tag{2.7}$$

$$|R/L\rangle = \frac{1}{\sqrt{2}}(|H\rangle \pm i|V\rangle) \tag{2.8}$$

In order to achieve the CHSH-Bell test we need first to measure the two-photon coincidence fringe visibility to verify the produced quantum entangled state and only later proceed with the S parameter measurement.

A careful analysis of errors is required in both quantities. For calculation of the standard deviation, the distribution goes towards a gaussian distribution for large n and therefore could be evaluated by error progression of the square roots of the measured quantities [§].

[§] To see an introduction to error analysis see [13].

2.3.1 Two-photon coincidence fringe visibility

The coincidence fringes are obtained via joint polarization measurements on the photon pairs; one polarizer A is set to a fixed angle α and the angle β of polarizer B is rotated from 0 to 2π. The number of coincident events $N(\alpha, \beta)$ detected behind the polarizers will exhibit sinusoidal fringes of the form $N(\alpha, \beta) = V \times \sin^2(\alpha - \beta)$, with a visibility

$$V = \frac{N_{max}(\alpha, \beta) - N_{min}(\alpha, \beta)}{N_{max}(\alpha, \beta) + N_{min}(\alpha, \beta)} \tag{2.9}$$

$N_{max/min}$ are the maxima/minima of the observed coincidences. Visibilities above 50% rule out a classical in favor of a quantum mechanical description of the electromagnetical fields of the photon pairs produced by parametric down-conversion, and $V > 1/\sqrt{2}$ allows the violation of a Bell inequality. However, to decide the question whether a quantum state is entangled or not, note that V can reach unity for product states measured in their σ_z basis. Therefore, one has to measure V in two conjugate basis, e.g. $(\alpha = 0, \alpha' = \pi/4)$ corresponding to (σ_z, σ_x) basis, to check whether a quantum state is entangled or not. To set the proper phase of a Bell state, consider that you can distinguish a $\phi^+(\psi^+)$ from a $\phi^-(\psi^-)$ and vice versa looking at different Pauli basis. This phase can be changed with the tilting of a non linear optical element, like a *BBO* used for compensation.

2.3.2 CHSH-Bell parameter

The correlation values (1.10) are related to the observed photon coincidence count rates $N(\alpha, \beta)$ measured along the four combinations of α, β and their orthogonal angles $\alpha_\perp, \beta_\perp$ via

$$E(\alpha, \beta) = \frac{N(\alpha, \beta) + N(\alpha_\perp, \beta_\perp) - N(\alpha, \beta_\perp) - N(\alpha_\perp, \beta)}{N(\alpha, \beta) + N(\alpha_\perp, \beta_\perp) + N(\alpha_\perp, \beta) + N(\alpha, \beta_\perp)} \tag{2.10}$$

To determine the Bell´s parameter (1.13) it´s then necessary to acquire coincidences for 16 different basis measurements. One possible angles set for achieving maximal violation consists of : $\{\alpha = 0°, \beta = 22,5°, \alpha' = 45°, \beta' = 67,5°\}$.

2.4 Alignment

In principle the alignment of the source means to move with the two collecting optics into the crossing points of idler and signal cones at degenerate wavelength. The angle between the pump beam and a cones intersection line is fixed at 3°. One can approximately position the coupler with the help of a pointer laser at this angle by sending the light in reverse direction. The two couplers are mounted on translation-stages, which makes it possible to move in horizontal and vertical plane. By placing an interference filter[¶] in front of the coupler only photons with degenerate wavelengths are passing.

The crystal is cut in such a way that by placing the crystal perpendicular with respect to pump beam direction, the angle between its optical axes and the pump is

[¶]Interference filters have the property to be transparent only for a narrow bandwidth at a designed wavelength.

θ. Fig. 2.4 shows how the cones (for degenerate case) change their sizes with respect to θ. Plotting the single photon count rates of each coupler arm versus θ, we can estimate which kind of misalignment exists. We can observe that the left arm sees two intensity peaks, this is an indicator for misalignment in vertical direction and we observe also a gap between left and right arm, which points on a misalignment in horizontal plane. By moving with the left coupler in vertical direction we can achieve that we just see one intensity peak, see fig. 2.4(b) and by moving with both couplers towards each other we align also for horizontal plane, see fig. 2.4(c). Due to the fact that we moved very close to the crossing points the coincident count rates increase. By putting polarization filters at H or V in front of the couplers, we can even work more precisely because we just see either idler or signal cones.

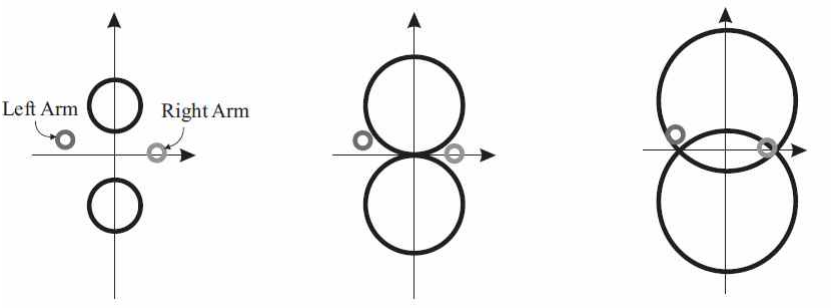

Figure 2.4: SPDC type-II degenerate case: for different angles of pump Θ_p the cones of idler and signal photons change size. The small circles represent the wrong position of the couplers. Figure from [15].

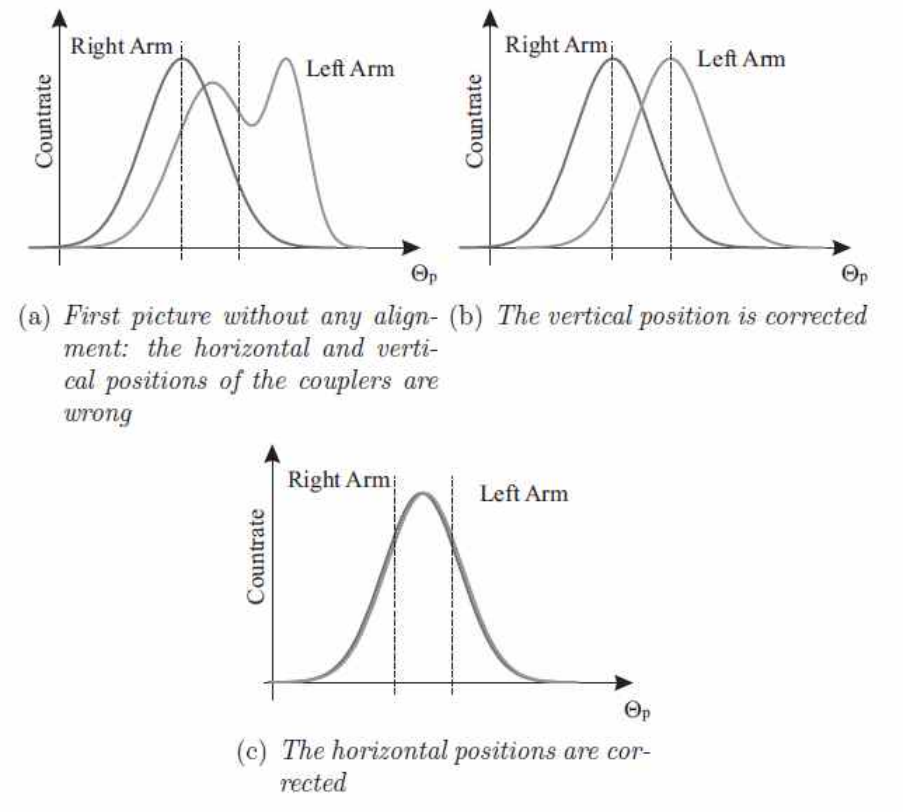

(a) *First picture without any alignment: the horizontal and vertical positions of the couplers are wrong*

(b) *The vertical position is corrected*

(c) *The horizontal positions are corrected*

Figure 2.5: With the help of interference filter we can look at degenerate photons. Figure from [15].

Bibliography

[1] L. Mandel and E. Wolf, *Optical Coherence and Quantum Optics* (Cambridge University Press, 1995).

[2] R. Prevedel, *Experimental all-optical one-way quantum computing* (Dissertation, 2008).

[3] A.Einstein, B.Podolsky, and N.Rosen. Can quantum-mechanical description of physical reality be considered complete? *Phys. Rev.*, 47:777780, 1935

[4] John S. Bell. On the einstein podalsky rosen paradox. *Physics*, 1(3):195-200, 1964.

[5] J.F. Clauser, M.A. Horne, A. Shimony, R.A. Holt (1969), Proposed experiment to test local hidden-variable theories, *Phys. Rev. Lett.* 23 (15): 880-4.

[6] A. Aspect, P. Grangier, and G. Roger, Experimental Realization of Einstein-Podolsky-Rosen-Bohm Gedankenexperiment: A New Violation of Bell's Inequalities. *Physical Review Letters*, Vol. 49, Iss. 2, pp. 91–94 (1982)

[7] Z.Y. Ou and L. Mandel. violation of Bell's inequality and Classical Probability in a Two-photon Correlation Experiment. *Physical Review Letters*, Vol 61, No. 1, pp 50-52 (1988).

[8] Paul G. Kwiat, Klaus Mattle, Harald Weinfurter, and Anton Zeilinger. New high-intensity source of polarization-entangled photon pairs. *Physical Review Letters*, 75(24):4337-4342,(1995)

[9] David J. Griths. Introduction to Quantum Mechanics. Prentice Hall, NJ, 1995.

[10] T. Scheidl *et al.*, Violation of local realism with freedom of choice, *PNAS*, 107, 10908 (2013).

[11] Marissa Giustina *et al.*, Bell violation using entangled photons wothout the fair-sampling assumption, *Nature* 497, 227 (2013).

[12] P. H. Eberhard. *Phys. Rev. A*, 1993.

[13] John R. Taylor. Introduction to Error Analysis. University Science Books, CA, second edition, 1997.

[14] S. Barz: *Eine Quelle polarisationsverschrrankter Photonenpaare im physikalischen Praktikum fur Fortgeschrittene.*. Staatsexamensarbeit, Universitat Mainz, 2008.

[15] Y. Nazirizadeh *Compact source for polarization entangled Photon Pairs*, Thesis, Max-Plank Institue, 2005.

[16] B. E.A. Saleh and M.C.Teich. *Fundamentals of Photonics.* 1994.

[17] D. Klyshko, *Photons and Nonlinear Optics* Gordon and Breach Science Publishers Ltd.,1988.

[18] B.A. Betchart *A Test of Bell's Inequality for the Undergraduate Laboratory*, Oberlin College, 2004

[19] Y.O.Lipp *Experimental realization of an interferometric quantum circuit to increase the computational depth*, Wien, 2011

[20] Y. Shih *Entangled biphoton source-property and preparation*, Rep. Prog. Phys. 66 (2003) 1009–1044.

[21] R. F. Werner, M. M. Wolf *Bell inequalities and Entanglement*, quant-ph/0107093 (2001)

Appendix A

Non-linear crystal : BBO

Type-II phase matching conditions produce a signal and idler with opposite polarizations (see main text 2.1.2).

To find the phase matching angles α and β for a signal/idler pair (see fig. A.1), first use $|\overrightarrow{k}| = \omega n/c$ and the approximation $n_o(\omega_s) \approx n_o(\frac{1}{2}\omega_p) \approx n_o(\omega_i)$ to rewrite eq. 2.5 as

$$\omega_s \sin\alpha + \omega_i \sin\beta = 0 \tag{A.1}$$

and

$$\omega_s \cos\alpha + \omega_i \cos\beta = \frac{\omega_p n_e(\omega_p, \theta)}{n_o(\frac{1}{2}\omega_p)}. \tag{A.2}$$

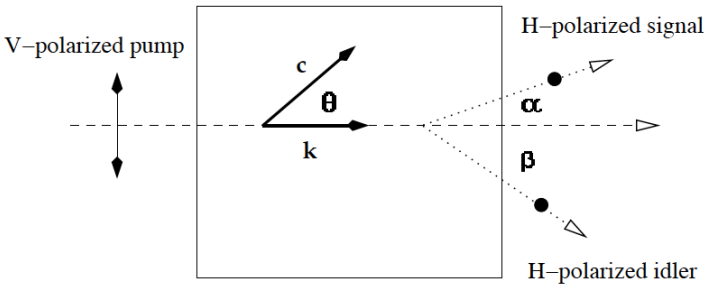

Figure A.1: A pump photon splits into signal and idler photons in type-I phase matched SPDC. Figure from [18].

For the degenerate case $\omega_s = \omega_i = \frac{1}{2}\omega_p$, it is clear that $\alpha = -\beta$. Substituting into the rewritten form of 2.5 yields

$$\frac{1}{n_e(\omega_p, \theta)} = \frac{\sec\alpha}{n_o(\frac{1}{2}\omega_p)}. \tag{A.3}$$

Combining this result with eq. 2.3 gives the relation between crystal cut, pump frequency, and phase matching angle

$$\frac{\sin^2(\theta)}{\overline{n}_e(\omega_p)^2} + \frac{\cos^2(\theta)}{n_o(\omega_p)^2} = \frac{\sec^2(\alpha)}{n_o(\frac{1}{2}\omega)}, \tag{A.4}$$

which can be solved explicitly given the indices of refraction.

BBO

Beta barium borate, also written β-BaB_2O_4 and *BBO*, is a common non-linear optical material. Its useful characteristics include transparency over a large bandwidth from UV through infrared, wide phase-matching capabilities, high damage threshold, and low hygroscopic susceptibility. Fig. A.2 shows some properties of BBO. Fig. A.3 graphs the Sellmeier equations for BBO's indices of refraction as a function of wavelength. Fig. A.4 shows a graph of eq. B.1 solved for BBO.

Crystal Structure	Trigonal
Crystal Symmetry	3m
Transmission Range	$0.2 - 3\mu m$
Damage threshold	$5\ GW/cm^2$
Birefringence	negative uniaxial
NLO d-coefficients $\left(\frac{pm}{V}\right)$	
	$d_{11} = 2.3$
	$d_{31} = 0.15$
Type-I	$d_{\text{eff}} = d_{31}\cos\theta$

Sellmeier equations (λ in μm)

$$n_e(\lambda)^2 = 2.7359 + \frac{0.01878}{\lambda^2 - 0.01822} - 0.01354\lambda^2$$

$$n_o(\lambda)^2 = 2.3753 + \frac{0.01224}{\lambda^2 - 0.01667} - 0.01515\lambda^2$$

Figure A.2: Properties of BBO.

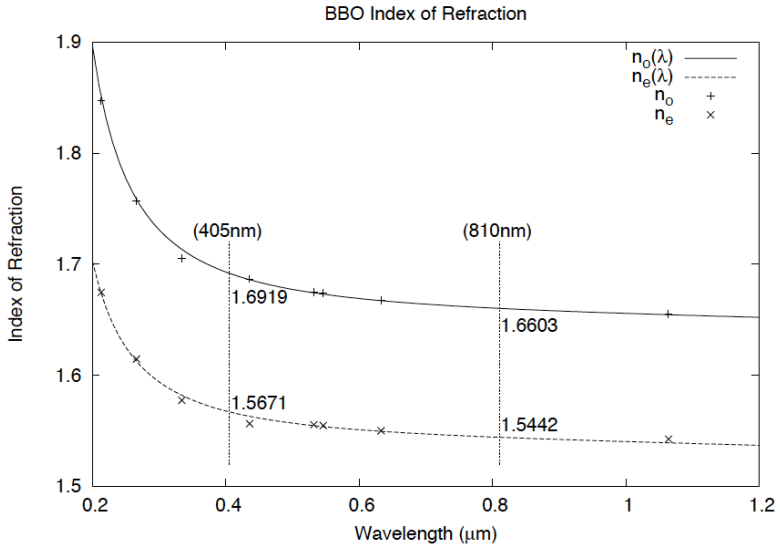

Figure A.3: The indices of refraction for BBO are given by the Sellmeier equations, shown in Table A.2

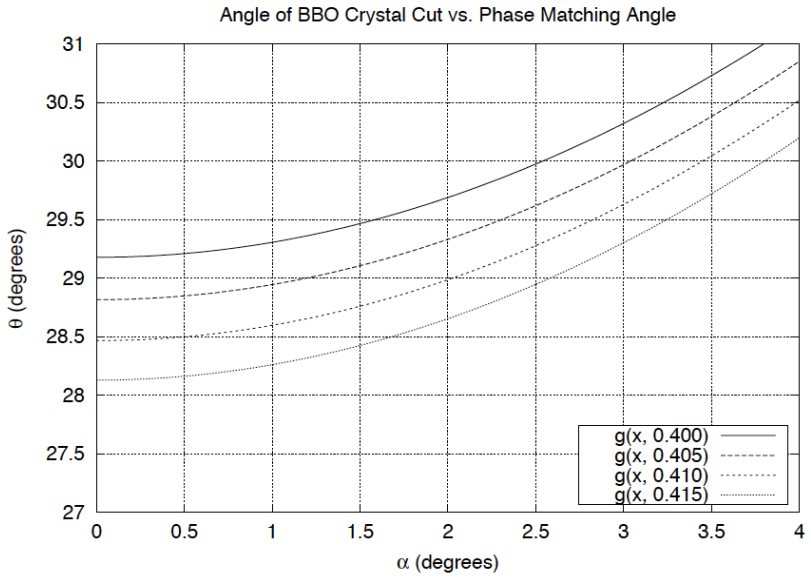

Figure A.4: BBO crystal cut as a function of the degenerate phase matching angle at pump wavelengths from 400*nm* to 415*nm*.

Appendix B

Gaussian Optics

To describe a beam we start from a paraxial solution of the Helmholtz equation. For the complex field amplitude of a beam we have the following expression

$$U(\vec{r}) = A_0 \frac{\omega_0}{\omega(z)} exp\Big[- \frac{\rho^2}{\omega(z)^2}\Big] exp\Big[- jkz - jk\frac{\rho^2}{2R(z)} + j\zeta(z)\Big] \tag{B.1}$$

where $\vec{r}$ is the position ($\vec{r} = (x, y, z)$) and $\rho = (x^2 + y^2)^{1/2}$ the radial distance to the center of the beam and z is the propagation direction. In equation B.1 the folllowing beam paramters are introduced

$$\omega(z) = \omega_0\Big[1 + \Big(\frac{z}{z_0}\Big)^2\Big]^{1/2} \tag{B.2}$$

$$R(z) = z\Big[1 + \Big(\frac{z_0}{z}\Big)^2\Big] \tag{B.3}$$

$$\zeta(z) = arctan\Big(\frac{z}{z_0}\Big) \tag{B.4}$$

$$\omega_0 = \Big(\frac{\lambda z_0}{\pi}\Big)^{1/2} \tag{B.5}$$

there $\omega(z)$ determines the distance ρ at which the field amplitude is reduced by a factor of $1/e$ in respect to its axial value at $\rho = 0$. We will refer to this parameter as the beam radius. The parameter ω_0 is the beam radius at $z = 0$ and is called waist size. $R(z)$ is the radius of the curvature of the wave front at the distance z. z_0 is defined as the *Rayleigth length*, this gives an approximation about the depth of the focus. We refer to equation B.1 as the fundamental gaussian beam, this solution is also called the TM_{00} mode. To follow the whole derivation one can use [16]. By following the derivation of equation B.1 one can see that q describes all properties of a gaussian beam

$$\frac{1}{q(z)} = \frac{1}{R(z)} - j\frac{\lambda}{\pi\omega^2(z)} \tag{B.6}$$

Gaussian Beam properties

Many interesting beam parameters can be derived from equation B.2 to B.5 and are discussed in the following. The optical intensity is given by the square of the

absolute value of complex field amplitude introduced in equation B.1

$$I(\rho, z) = I_0\Big[\frac{\omega_0}{\omega(z)}\Big]^2 exp\Big[-\frac{2\rho^2}{\omega^2(z)}\Big] \tag{B.7}$$

From this formula we can calculate the intensity distribution of a gaussian beam at any distance z (figure 3.1(a)). By looking more close to equation B.7 and (figure 3.1(a)) we will see the gaussian behavior, which gives the name Gaussian optics. We define also the $\omega_{FWHM}(z)$* which is the diameter of the beam where the intensity is half of the maximum intensity. To investigate how the beam radius behaves in z-direction we can plot w(z) according to B.2 and will see that if we are far enough from the center of the beam the beam radius grows linearly (figure 3.1(b)). This happens for z bigger than the Rayleigh length z_0. The angle of the beam radius is then

$$\theta = \frac{\lambda}{\pi\omega_0} \tag{B.8}$$

We refer to this angle as the divergence of the beam. At $z = z_0$ the curvature of the wavefront decreases to its minimum value. This we see if we plot the wavefront curvature $R(z)$ introduced in B.3. We also see that $R(0)$ is infinite, this means that at $z = 0$ we have a plane wavefront. To define and work with a theoretical gaussian beam the wavelength and the waist size are sufficient parameters. In case of a real beam, however, we have to deal with an additional parameter, namely the M^2-Factor.

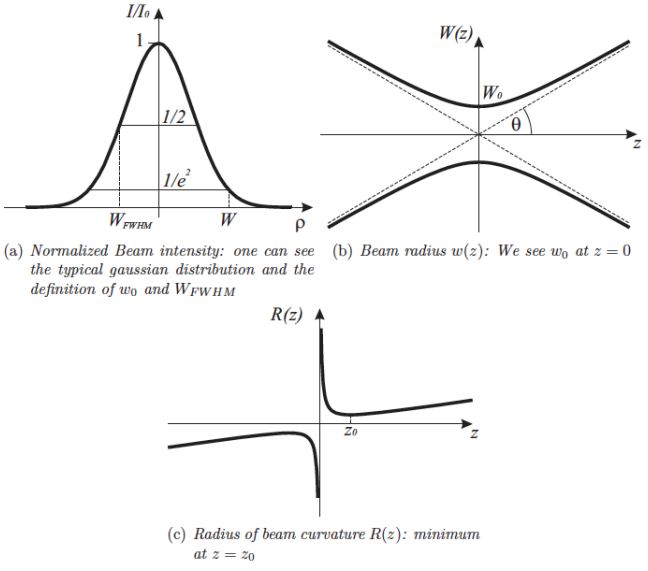

(a) *Normalized Beam intensity: one can see the typical gaussian distribution and the definition of w_0 and W_{FWHM}*

(b) *Beam radius $w(z)$: We see w_0 at $z = 0$*

(c) *Radius of beam curvature $R(z)$: minimum at $z = z_0$*

Figure B.1: Gaussian beam profiles

M^2-Factor

Unfortunately a real-life laser does not provide true zero order gaussian mode, but also higher order modes. To have a measure for it the M^2-Factor is introduced. The M^2-Factor† defines a value which characterizes the differences between an theoretical

*FWHM stands for Full Width at Half Maximum

†real beam $M^2 \geq 1$, perfect gaussian beam $M^2 = 1$

gaussian beam like defined in equation B.1 and a real beam. The diameter of the real beam at every distance is M times larger than the diameter of the theoretical gaussian beam:

$$\omega_{REAL}(z) = \omega(z)M \tag{B.9}$$

From equation B.9 and B.2, B.5 we can derive the parameter which are interesting for us like

$$\omega_{REAL}(z) = \omega_0\Big[1 + \Big(\frac{z\lambda M^2}{\pi\omega_0^2}\Big)^2\Big]^{1/2} \tag{B.10}$$

$$\theta_{REAL} = \lambda\frac{M^2}{\pi\omega_0} \tag{B.11}$$

One of the ways to determine the M^2 experimentally is by measuring the beam radius at different distances. Equation B.10 can be fitted to the measured data and one can estimate the M^2. As we will see a real beam may also have different M^2 in horizontal and vertical planes. Also other beam asymmetries can be observed like Astigmatism and *Asymmetric Waist*. Astigmatism means that the waist do not have the same position, whereas different sizes of waist is called by Asymmetric Waist. Once the M^2-factor is known one can analytically describe the propagation of the beam through any optical system. This issue is addressed in the next section.

Gaussian Transformation

By passing an optical system like a lens the parameters of a gaussian beam, like the waist size and waist position, are generally changed. We will refer to this fact as *gaussian transformation*. One of the most common ways to describe a gaussian transformation is by using the ABCD law. The advantage of this method is that the same matrices as used as in matrix optics, which are introduced in the next section. The transformation is done on the q-parameter of the incident beam

$$q_2 = \frac{Aq_1 + B}{Cq_1 + D}, \tag{B.12}$$

where q_1 is the incident gaussian beam defined like equation B.6 and q_2 is the transmitted gaussian beam.

Raytracing

Raytracing via matrix optics is one of the most general ways to treat paraxial rays [‡]. Each ray is described by its radial position a and its angle α relative to the optical axis. These variables change by passing an optical system due to Snell´s law or geometries. The new position a and angle α are determined using the following transformation

$$\begin{pmatrix} a' \\ \alpha' \end{pmatrix} = M\begin{pmatrix} a \\ \alpha \end{pmatrix}$$

where M is a 2×2 *ray transfer matrix* with elements A, B, C and D which uniquely characterizes any optical element. In case of a ray passing free space the transfer

[‡]rays propagating under a small angle (such that $sin\theta \approx \theta$) with respect to optical angle are called paraxial rays

matrix is the following

$$\begin{pmatrix} 1 & d \\ 0 & 1 \end{pmatrix},$$

where d is the free space length. The matrix for a lens looks the following

$$\begin{pmatrix} 1 & 0 \\ \frac{-1}{f} & 1 \end{pmatrix},$$

where f is the focal length of the lens. The transfer matrix of a composed system consisting of more than one component is calculated by multiplying all the transfer matrices of each component.

Appendix C

Waveplates

The polarization state of photons can be manipulated with wave plates. Commonly made of uniaxial birefringent crystals, they induce a relative phase shift between the (linear) polarization component aligned with the ordinary and the extraordinary axis

$$\Delta\phi = \frac{2\pi}{\lambda} d(|n_o - n_e|), \tag{C.1}$$

where the thickness d can be set. Note that there is a dependence on the wavelength limiting the intended effect to a certain spectral range. Mostly, two kinds of wave plates are used: half-wave plates (HWP) and quarter-wave plates (QWP); introducing a phase shift of $\Delta\phi = \pi$ and $\Delta\phi = \frac{\pi}{2}$, respectively. Rotating the wave plate in the plain perpendicular to the incident light corresponds to a change in basis and affects how the polarization amplitudes are split. The effect of HWP and QWP can be written as unitary operators

$$U_{HWP}(\theta) = e^{i\frac{\pi}{2}} \begin{pmatrix} \cos 2\pi & \sin 2\pi \\ \sin 2\pi & -\cos 2\pi \end{pmatrix}, \tag{C.2}$$

$$U_{QWP}(\theta) = \frac{1}{\sqrt{2}} \begin{pmatrix} 1 + i\cos 2\pi & i\sin 2\pi \\ i\sin 2\pi & 1 - i\cos 2\pi \end{pmatrix}, \tag{C.3}$$

where the angle θ denotes the orientation of the optical axis with respect to horizontal polarization. Their property to alter the polarization state of a photon makes them suitable for implementing single-qubit unitaries. An arbitrary single-qubit unitary operation U can be decomposed into a combination of three wave plates

$$U = U_{QWP}(\gamma) U_{HWP}(\beta) U_{QWP}(\alpha). \tag{C.4}$$

To transform any polarization state to H or V , two wave plates, a QWP and a HWP, are enough

$$U_{\rightarrow H/V} = U_{HWP}(\beta) U_{QWP}(\alpha). \tag{C.5}$$

The QWP brings a potentially elliptical state to the x-z plane, where states with linear polarization are situated. For these states applying a HWP corresponds to a rotation about the y axis and can thus map any such state to H/V . Fig . C.1 lists the required angles for some common polarizations.

$Input \rightarrow$	QWP	HWP	$\rightarrow Output$
H/V	$0°$	$0°$	H/V
D/A	$45°$	$22.5°$	H/V
R/L	$45°$	$45°$	H/V

Figure C.1: How to transform standard bases to the H/V basis using a QWP and a HWP. Note that QWP and HWP do not commute, so the angles are specific to the given order.

Before a wave plate can be used the position of the optical axis needs to be determined.

Tip *Aligning a wave plate. Place an unknown wave plate between two PBSs and monitor the intensity, while rotating it in the plain perpendicular to the incident light. For some angle the intensity reaches a minimum: (HWP) when the polarization is flipped from H to V ; (QWP) the linear polarization is transformed to circular polarization. Attention must be given that all QWPs are aligned to the same axis, ordinary or extraordinary. Use a reference QWP: two QWPs aligned to the same axis will act as an effective HWP, while compensating each other when not.*